Energy & Environmental Science

COMMUNICATION

View Article Online
View Journal | View Issue

Cite this: *Energy Environ. Sci.*, 2014, 7, 2981

Received 17th April 2014
Accepted 14th July 2014

DOI: 10.1039/c4ee01220h

www.rsc.org/ees

Low band gap *S,N*-heteroacene-based oligothiophenes as hole-transporting and light absorbing materials for efficient perovskite-based solar cells†

Peng Qin,‡[a] Hannelore Kast,‡[b] Mohammad K. Nazeeruddin,[a] Shaik M. Zakeeruddin,[a] Amaresh Mishra,*[b] Peter Bäuerle[b] and Michael Grätzel*[a]

Novel low band gap oligothiophenes incorporating *S,N*-heteropentacene central units were developed and used as hole-transport materials (HTMs) in solid-state perovskite-based solar cells. In addition to appropriate electronic energy levels, these materials show high photo-absorptivity in the low energy region, and thus can contribute to the light harvesting of the solar spectrum. Solution-processed $CH_3NH_3PbI_3$-based devices using these HTMs achieved power conversion efficiencies of 9.5–10.5% in comparison with 7.6% obtained by reference devices without HTMs. Photoinduced absorption spectroscopy gave further insight into the charge transfer behavior between photoexcited perovskites and the HTMs.

Broader context

Organic–inorganic hybrid photovoltaic devices have attracted considerable research interest in recent years as a competitive alternative to inorganic solar cells. In this respect, organo-lead halide perovskites have emerged as excellent light absorbers reaching remarkable power conversion efficiencies over 15% using wide band gap hole transport materials (HTMs). On the other hand, low band gap p-type conjugated oligomers have shown excellent performance in organic solar cells due to their strong absorption, good charge transport properties and tunable HOMO/LUMO energy levels. In this work, we have developed new acceptor–donor–acceptor (A–D–A)-type π-extended oligomers exhibiting strong absorption in the low energy region. Due to their high absorption coefficients and appropriate energy levels they were utilized as HTMs in perovskite based solar cells exhibiting promising power conversion efficiencies up to 10.5%. Most importantly, the results demonstrate that these oligomers are also contributing to the light absorption forming dual absorber system together with the perovskite. Promising development in this direction is expected in the future.

Recently, organic–inorganic hybrid systems based on organometal halide perovskites with the general formula $(RNH_3)MX_3$ (R = alkyl, M = Pb, X = I, Br or Cl) have aroused considerable success as light harvesters in solid-state heterojunction solar cells.[1–9] Their optoelectronic properties can be easily tuned by changing the alkyl substituent at the ammonium cation as well as by variation of the halogen atoms. These perovskite nanoparticles possess direct band gaps, large absorption coefficients, and high charge carrier mobilities. In 2009,[2a] perovskites have been employed for the first time as sensitizers in photoelectrochemical cells using liquid electrolytes achieving power conversion efficiencies (PCE) of 3.8–6.5%.[2] However, the device performance was dramatically reduced due to the dissolution of the perovskite in the electrolyte. This problem was solved by using 2,2′,7,7′-tetrakis(*N*,*N*-di-*p*-methoxyphenylamino)-9,9′-spirobifluorene (spiro-MeOTAD) as a solid state hole transport material (HTM), generating a PCE of 9.7–12.3%.[3,4] In these devices, the perovskite was deposited onto mesoporous TiO_2 (mp-TiO_2) or Al_2O_3 scaffolds by one step deposition from a solution of PbX_2 and CH_3NH_3X in an appropriate solvent. Later on, the PCEs have been dramatically improved to over 15% by sequential deposition of PbX_2 and CH_3NH_3X either from solution or by vacuum-techniques to form the $CH_3NH_3PbX_3$ perovskite.[6–8] In all these contributions, the HTMs used were mainly wide band gap spiro-MeOTAD or poly(triarylamine) (PTAA),[9a,b] which in fact showed good hole mobilities, but almost no absorption in the visible and near-IR region of the solar spectrum. In this respect, low band gap donor–acceptor (D–A) polymers with strong absorption in this spectral region, well-known from bulk-heterojunction solar cells,[10] have been used as HTMs in $CH_3NH_3PbX_3$-based perovskite solar cells exhibiting PCEs of 4.2–9.2%.[9] In these devices, the D–A polymers[9] or oligomers[11] served as hole-transporters, whereas the perovskite played the role of the light absorber.

In this work, we report the synthesis and characterization of two novel A–D–A-type oligomers **1** and **2** incorporating a rigid *S,N*-heteropentacene central unit and their use as HTMs in

[a]*Laboratory of Photonics and Interfaces, Institute of Chemical Sciences and Engineering, École Polytechnique Fédérale de Lausanne (EPFL), Station 6, CH-1015 Lausanne, Switzerland. E-mail: michael.graetzel@epfl.ch*

[b]*Institute of Organic Chemistry II and Advanced Materials, Ulm University, Albert-Einstein-Allee 11, 89081 Ulm, Germany. E-mail: amaresh.mishra@uni-ulm.de*

† Electronic supplementary information (ESI) available: Experimental details, characterization methods, ^1H and ^{13}C NMR and HR-MS spectra, devices fabrication conditions and measurements. See DOI: 10.1039/c4ee01220h

‡ These authors contributed equally to this work.

efficient solid-state perovskite-based solar cells. These class of materials act as good hole transporters,[12] which simultaneously strongly absorb light in the visible and near-infrared region. The high light harvesting ability of the oligomers can have additional contribution to the photocurrent generation of the perovskite solar cells, which were fabricated by sequential solution-processed deposition.[6] Excellent PCEs 10.5% and 9.5% were achieved for **1** and **2**, respectively, in comparison with 7.6% for devices without hole transporters. These soluble HTMs as well allow for fine-tuning of the frontier orbital energies by variation of the linkers between the central thiophene–pyrrol-based *S*,*N*-heteropentacene and the terminal dicyanovinylene (DCV) acceptor groups, thus contributing to the effective charge transport and the photocurrent enhancement in the device.

The synthetic routes to oligomers **1** and **2** are displayed in Scheme 1. The key building block 3,3′,3″,4′-tetrabromo-2,2′:5′,2″-terthiophene **5** was prepared by Pd-catalyzed Negishi-coupling of (3-bromothien-2-yl)zinc(II) chloride **4** (2.5 eq.) and tetrabromothiophene **3** (ref. 13) in 75% yield. Pd-catalyzed tandem Buchwald–Hartwig coupling of **5** with 2-ethylhexyl amine afforded ring-fused *S*,*N*-heteropentacene **6** in 60% yield. The corresponding bis-stannylated derivative **7** was obtained by lithiation of **6** with *n*-BuLi followed by quenching with trimethyltin chloride. A–D–A-oligothiophenes **1** and **2** were finally synthesized by Pd-catalyzed Stille-type coupling of **7** with dicyanovinylene (DCV)-substituted iodothiophene **8** and iodobithiophene **9** in yields of 80% and 82%, respectively.

The UV-vis absorption spectra of **1** and **2** in dichloromethane solution are shown in Fig. 1 and data are summarized in Table 1. Oligomer **1** showed an intensive charge-transfer (CT) absorption band with a maximum at 655 nm and a high molar extinction coefficient (117 600 M^{-1} cm^{-1}), whereas the CT-band of the longer oligomer **2** is blue-shifted to 630 nm and less intense (86 300 M^{-1} cm^{-1}) due to the more flexible bithiophene units in **2**. In addition, a higher energy band at 380 nm was observed for **1**, which becomes intense and red-shifted to 430 nm by replacing the thiophene unit by the bithiophene unit in **2**. The absorption bands of **1** and **2** coated on TiO_2 films are significantly red-shifted to 725 and 675 nm, respectively. The optical band gaps (E_g^{opt}) for **1** and **2** in thin films were about 0.16 eV and 0.18 eV lower compared to the band gaps obtained from solution spectra. Unlike spiro-MeOTAD and PTAA, which mainly absorb below 400 nm, oligomers **1** and **2** have strong light absorption in the visible to near-IR region. Thus they can play a role as a light absorber in the long wavelength region where the perovskite absorption is very low.

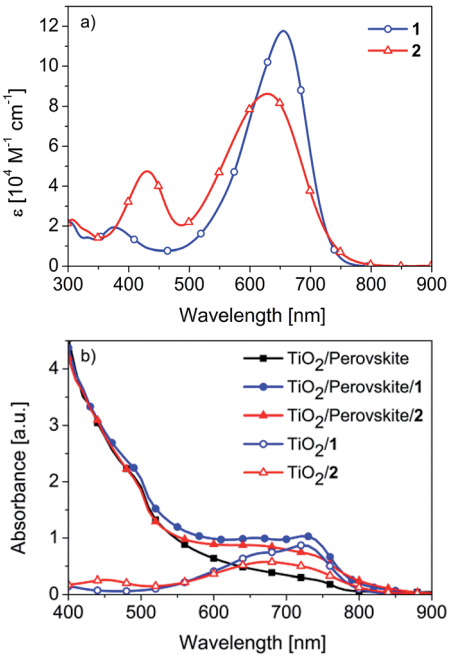

Fig. 1 UV-vis absorption spectra of (a) **1** and **2** in dichloromethane solution and (b) **1** and **2** coated on mesoporous TiO_2 and TiO_2/perovskite films. A TiO_2/perovskite film without HTMs is shown for comparison.

To further investigate the contribution of light absorption from the HTMs **1** and **2**, the UV-vis spectra of perovskite films on TiO_2 with and without HTMs were recorded. As shown in Fig. 1b, the perovskite itself has strong absorption in the visible region at 400 nm, which continuously drops and becomes weaker after 600 nm. In contrast, both oligomers **1** and **2** have strong absorption between 600–800 nm, which is complementary to the perovskite. We note that in the presence of oligomers, $TiO_2/CH_3NH_3PbI_3$/HTM films showed a significant enhancement in the absorption between 550–800 nm. This additional absorption in the low energy region is attributed to the oligomers.

In cyclic voltammetry measurement two $1e^-$-oxidation waves were observed for oligomers **1** and **2**, which are assigned to the formation of stable radical cations and dications, typical for an oligothiophene backbone. The irreversible $2e^-$-reduction wave corresponds to the simultaneous one-electron transfer to the terminal DCV groups (Table 1, Fig. S1†).[14] The oxidation potentials for **2** are negatively shifted by 190 mV and 300 mV compared to **1** due to the elongated conjugated π-system. The highest occupied molecular orbital (HOMO) and lowest unoccupied molecular orbital (LUMO) energy levels of oligomers **1** and **2** were determined from the onset of the first oxidation and reduction wave, respectively (Table 1, Fig. 2a). Thereby, the HOMO energies of both oligomers **1** and **2** are suitable for their

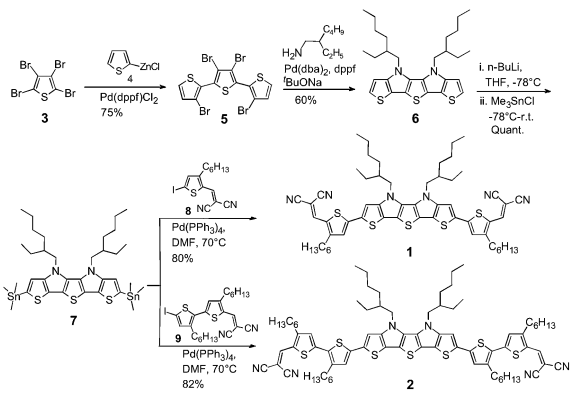

Scheme 1 Synthesis of π-conjugated oligomers **1** and **2**.

Table 1 Optoelectronic properties of oligomers **1** and **2**

Oligomer	λ_{abs}^{max} [nm] soln.	ε_{max} [M^{-1} cm^{-1}]	E_g^{opt} [eV] soln.	λ_{abs} [a] [nm] film	E_g^{opt} [a] [eV] film	E_{ox1}^0 [V]	E_{ox2}^0 [V]	E_{red1}^0 [V]	E_{HOMO} [b] [eV]	E_{LUMO} [b] [eV]	E_g^{CV} [eV]
1	655	117 600	1.70	725	1.54	0.23	0.77	−1.33	−5.26	−3.77	1.49
2	630	86 300	1.68	675	1.50	0.04	0.47	−1.36	−5.10	−3.74	1.36

[a] The film of oligomers coated on mp-TiO_2. [b] Calculated from the onset of the respective redox waves; Fc/Fc^+ was set to −5.1 eV *vs.* vacuum.

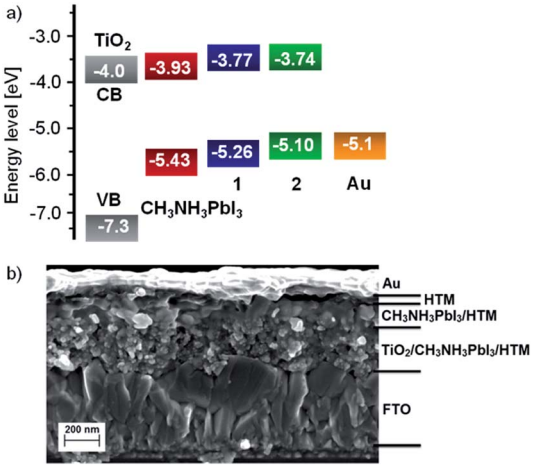

Fig. 2 (a) Energy level diagram of the components used in solar cells described. (b) Cross-sectional SEM image of a complete device.

use as HTMs in perovskite heterojunction solar cells containing $CH_3NH_3PbI_3$ as a light harvester and mp-TiO_2 as an electron transport layer. In comparison with **2**, the lower HOMO energy level of **1** is expected to result in a higher open-circuit voltage (V_{OC}), because the V_{OC} depends on the difference between the HOMO level of the HTM and the quasi-Fermi level of TiO_2. In addition, the LUMO energies lie in an ideal regime relative to the LUMO of the perovskite and should provide a sufficient driving force for charge separation at the oligomer/perovskite interface.

The hole transport properties of oligomers **1** and **2** were determined from hole-only devices using the space charge limited current (SCLC) model. The extracted hole mobilities for **1** and **2** are 7.3×10^{-5} cm^2 V^{-1} s^{-1} and 6.6×10^{-5} cm^2 V^{-1} s^{-1}, respectively (Fig. S2, ESI†).

For the device preparation, the deposition of $CH_3NH_3PbI_3$ on mp-TiO_2 films was performed in two steps by spin-coating a 1.3 M PbI_2 solution in *N*,*N*-dimethylformamide (DMF) and subsequent dip-coating of the TiO_2/PbI_2 film into a solution of CH_3NH_3I in 2-propanol. The dip-coating process resulted in the conversion of the two components into the $CH_3NH_3PbI_3$ perovskite. After annealing the perovskite film, HTMs **1** or **2** (30 mM) were deposited by spin-coating from tetrachloroethane at 60 °C. As seen from the top-view scanning electron microscopy (SEM) image, there is a uniform distribution of $CH_3NH_3PbI_3$ crystals over the surface of the mesoporous TiO_2 photoanode. After depositing the HTM, the $CH_3NH_3PbI_3$ crystals are uniformly covered (Fig. S3, ESI†). The cross-sectional SEM image further shows that the HTM penetrate into the remaining space of the pores in the TiO_2/perovskite layer and at the same time form a thin capping layer on the top (Fig. 2b). Finally, the devices were completed by evaporation of a thin gold layer as the back contact.

Fig. 3a shows the current–voltage (*J*–*V*) characteristics of solar cells based on the structure FTO/compact-TiO_2/mp-TiO_2/$CH_3NH_3PbI_3$/oligomer **1** or **2**/Au. A reference cell without any HTM was prepared for comparison, which displayed a short-circuit current density (J_{SC}) of 14.0 mA cm^{-2}, a V_{OC} of 790 mV, and a fill factor (FF) of 0.69, resulting in a PCE of 7.6%. The average PCE of five identical devices without HTMs is 6.9 ± 0.5% (Table S1†). The use of oligomers **1** and **2** as HTMs substantially increased the PCE of the most efficient devices to 10.5% for **1** and 9.5% for **2** under standard global AM 1.5 illumination. The excellent overall improvement came from a significant increase of the J_{SC} (16.4 and 15.2 mA cm^{-2}) and V_{OC} (992 and 900 mV) values, whereas the FF only marginally differed (Table 2). The 92 mV higher V_{OC} for oligomer **1** compared to **2** comes from the lower HOMO energy level and the higher J_{SC} mainly due to efficient charge transport process.

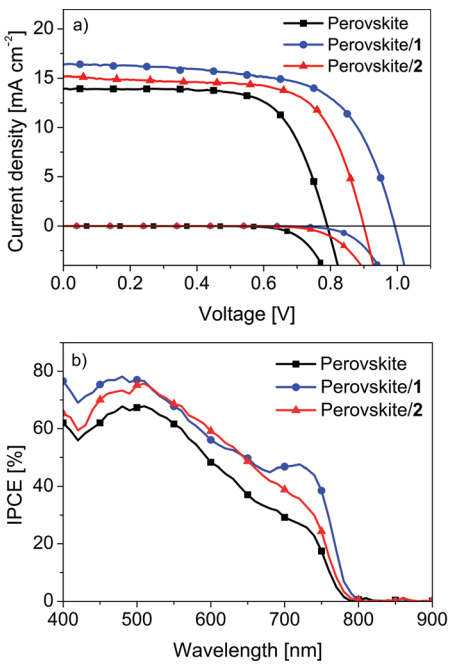

Fig. 3 *J*–*V* characteristics (a) and IPCE spectra (b) of the heterojunction solar cells based on HTMs **1** and **2**, and a reference cell without HTMs.

Table 2 Photovoltaic parameters of $CH_3NH_3PbI_3$-based heterojunction solar cells containing oligomers **1** and **2** as HTMs

Oligomer HTM	J_{SC} [mA cm^{-2}]	V_{OC} [mV]	FF	PCE [%]
1	16.4	992	0.65	10.5
2	15.2	900	0.68	9.5
No HTM	14.0	790	0.69	7.6

The obtained PCEs are much higher compared to the low band gap polymers reported in the literature.[9]

In Tables S2 and S3† we summarize the statistical data on a batch of ten identical devices for oligomers **1** and **2**, giving the average PCE values of 10.0 ± 0.4% and 8.9 ± 0.5%, respectively. The small standard deviation points towards good device reproducibility.

Fig. 3b shows the incident-photon-to-current conversion efficiency (IPCE) spectra for the perovskite cells with and without HTMs. The photocurrent generation starts at around 800 nm, in agreement with the band gap (E_g = 1.55 eV) of $CH_3NH_3PbI_3$, and reaches a peak IPCE value of around 68% at 510 nm for the device without a hole-transporter. The use of oligomers **1** and **2** as HTMs gave a noticeable improvement of the photocurrent over the whole region between 400 to 800 nm due to more effective charge extraction and/or light harvesting. Most importantly, the contribution of oligomer **1** to the photocurrent can clearly be seen as an additional band between 680–800 nm with IPCE values of 48% at 720 nm which is correlated well with the absorption maximum in thin films (Fig. 1b). The integrated current densities from the IPCE spectra for devices **1**, **2** and without HTMs were 15.3, 14.4, and 12.4 mA cm^{-2}, respectively. Thus, there is good agreement of the measured J_{SC} with the IPCE spectra, showing that the spectral mismatch between the simulator used as the light source and the solar emission spectrum is below 5%.

The light harvesting efficiency (LHE) and absorbed photon-to-current conversion efficiency (APCE) spectra were determined with and without HTMs (Fig. S4 and S5, ESI†). The LHEs were nearly identical between 400–550 nm, since the light harvesting mainly comes from the perovskite. After 550 nm, the LHEs are significantly higher with the presence of HTMs **1** and **2**. This result clearly demonstrated that the HTMs also contribute to the light harvesting together with the perovskite. However, the APCEs with HTM **2** are lower between 650–750 nm. Since in the longer wavelength region, more excitons will be generated in the HTM instead of perovskite. In comparison with HTM **1**, with the presence of HTM **2** the charges cannot be extracted effectively. The lower APCEs between 650–750 nm give the reason why no clear peak corresponding to HTM **2** appears in the IPCE spectrum.

In order to further clarify the light absorbing ability of the HTMs we have prepared devices with a cell structure of TiO_2/HTM **1** or **2**/Au without perovskites. The devices showed lower J_{SC} and V_{OC} values with HTM **2** (Fig. S6, Table S4, ESI†). The results indicated that the HTMs **1** and **2** could work as light harvesters and the charge separation occurs between TiO_2 and HTMs. The low performance is mainly due to the limitation of material loading during the spin-coating process and the fast charge recombination between TiO_2 and the oligomer.

The charge generation in the whole device was further examined by photoinduced absorption spectroscopy (PIA). Fig. 4a shows PIA spectra of mp-TiO_2 films coated with perovskite, HTM **1**, and with both. For the perovskite alone, we observed features in the near IR region which are assigned to the electrons injected into TiO_2,[15] and a negative band between 700–850 nm due to the emission of perovskite itself. A TiO_2/**1** film without perovskites showed a negative band at wavelengths shorter than 870 nm and a positive band beyond 950 nm due to the ground state bleaching and absorption of the oxidized species (assigned to the radical cation located on the donor moieties) of **1** after photoexcitation. This result indicates that charge separation occurs between TiO_2 and oligomer **1** even without the presence of perovskites. In the presence of a perovskite layer, the absorption features of the oxidized species of **1** are stronger extending from 800–1400 nm. At the same time, the negative band from the emission of the perovskite is quenched. A similar phenomenon was also observed for oligomer **2**. The PIA-results demonstrate that effective charge transfer takes place between the photoexcited perovskite and HTM **1** and **2** under formation of long-lived charged species.

At this point, we would like to emphasize that high performance devices comprising perovskite/HTMs **1** and **2** combinations can be prepared without the use of any additives, such as lithium bis(trifluoromethyl sulfonyl)imide (LiTFSI), 4-*tert*-butylpyridine (TBP) or even dopants, which are typically used in the case of spiro-MeOTAD or semiconducting polymers in order to get higher efficiencies.[8,10,16]

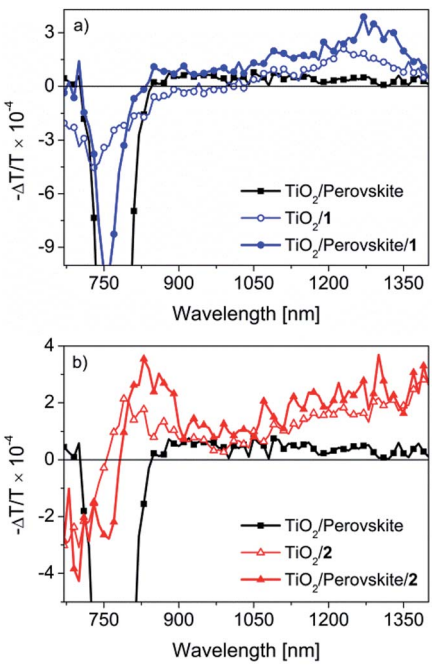

Fig. 4 PIA spectra of mp-TiO_2 films coated with perovskite, oligomer **1**, and perovskite/**1** (a) and with perovskite, oligomer **2**, and perovskite/**2** (b). Excitation wavelength: λ_{ex} = 642 nm.

Conclusions

In conclusion, novel low band gap A–D–A-type oligothiophenes **1** and **2** comprising electron-rich thiophene-pyrrole-based *S*,*N*-heteropentacene central units and terminal dicyanovinylene acceptor groups were developed. The strongly red-shifted absorption and appropriate frontier orbital energy levels of the oligomers prompted us to use them as HTMs in $CH_3NH_3PbI_3$-based photovoltaic devices. Solution-processed heterojunction solar cells fabricated with the new HTMs **1** and **2** and without any additives yielded excellent power conversion efficiencies of 10.5% and 9.5%, respectively. Besides acting as a HTM, we also see a contribution of oligomer **1** to the light absorption in the low energy region of the solar spectrum forming a dual light absorbing system with the perovskite, which opens up a new avenue for the fabrication and material selection of perovskite-based devices. Photoinduced absorption spectroscopic studies clearly demonstrated the effective charge transfer between the photoexcited perovskite and the HTMs. The present findings demonstrate that the appropriate combination of conjugated building blocks can lead to light harvesting organic semiconductors that have suitable frontier orbital energy levels for use as hole transporting materials in perovskite-based solar cells. It is anticipated that with fine-tuning of molecular structures in combination with optimized device processing conditions further improvement in solar cell performance is possible.

Acknowledgements

A.M., H.K., and P.B. thank the German Federal Ministry of Education and Research (BMBF) for financial support in the frame of joint project LOTsE. P.Q., M.K.N., S.M.Z., and M.G. acknowledge financial contribution from Greatcell Solar SA, Epalinges, Switzerland, the King Abdullah University of Science and Technology (KAUST, Award no. KUS-C1-015-21), the European Community's Seventh Framework Programme "CE-Mesolight" EPFL ECR advanced grant agreement no. 247404. M.K.N. thanks the Global Research Laboratory (GRL) Program, Korea, and World Class University programs (Photovoltaic Materials, Department of Material Chemistry, Korea University) funded by the Ministry of Education, Science and Technology through the National Research Foundation of Korea (no. R31-2008-000-10035-0). The authors thank Dr Peng Gao for the synthesis of CH_3NH_3I and Dr Nicolas Tetreault for the Cross-sectional SEM measurement.

Notes and references

1 For recent reviews: (*a*) H. J. Snaith, *J. Phys. Chem. Lett.*, 2013, **4**, 3623–3630; (*b*) N.-G. Park, *J. Phys. Chem. Lett.*, 2013, **4**, 2423–2429; (*c*) J. H. Rhee, C.-C. Chung and E. W.-G. Diau, *NPG Asia Mater.*, 2013, **5**, e68, DOI: 10.1038/am.2013.1053; (*d*) S. Kazim, M. K. Nazeeruddin, M. Grätzel and S. Ahmad, *Angew. Chem., Int. Ed.*, 2014, **53**, 2812–2824; (*e*) P. P. Boix, K. Nonomura, N. Mathews and S. G. Mhaisalkar, *Mater. Today*, 2014, **17**, 16–23.

2 (*a*) A. Kojima, K. Teshima, Y. Shirai and T. Miyasaka, *J. Am. Chem. Soc.*, 2009, **131**, 6050–6051; (*b*) J.-H. Im, C.-R. Lee, J.-W. Lee, S.-W. Park and N.-G. Park, *Nanoscale*, 2011, **3**, 4088–4093.

3 H.-S. Kim, C.-R. Lee, J.-H. Im, K.-B. Lee, T. Moehl, A. Marchioro, S.-J. Moon, R. Humphry-Baker, J.-H. Yum, J. E. Moser, M. Grätzel and N.-G. Park, *Sci. Rep.*, 2012, **2**, 591, DOI: 10.1038/srep00591.

4 (*a*) M. M. Lee, J. Teuscher, T. Miyasaka, T. N. Murakami and H. J. Snaith, *Science*, 2012, **338**, 643–647; (*b*) J. M. Ball, M. M. Lee, A. Hey and H. J. Snaith, *Energy Environ. Sci.*, 2013, **6**, 1739–1743.

5 (*a*) L. Etgar, P. Gao, Z. Xue, Q. Peng, A. K. Chandiran, B. Liu, M. K. Nazeeruddin and M. Grätzel, *J. Am. Chem. Soc.*, 2012, **134**, 17396–17399; (*b*) J. Shi, J. Dong, S. Lv, Y. Xu, L. Zhu, J. Xiao, X. Xu, H. Wu, D. Li, Y. Luo and Q. Meng, *Appl. Phys. Lett.*, 2014, **104**, 063901.

6 (*a*) J. Burschka, N. Pellet, S.-J. Moon, R. Humphry-Baker, P. Gao, M. K. Nazeeruddin and M. Grätzel, *Nature*, 2013, **499**, 316–319.

7 M. Liu, M. B. Johnston and H. J. Snaith, *Nature*, 2013, **501**, 395–398.

8 D. Liu and T. L. Kelly, *Nat. Photonics*, 2014, **8**, 133–138.

9 (*a*) J. H. Heo, S. H. Im, J. H. Noh, T. N. Mandal, C.-S. Lim, J. A. Chang, Y. H. Lee, H.-j. Kim, A. Sarkar, M. K. Nazeeruddin, M. Grätzel and S. I. Seok, *Nat. Photonics*, 2013, **7**, 486–491; (*b*) J. H. Noh, S. H. Im, J. H. Heo, T. N. Mandal and S. I. Seok, *Nano Lett.*, 2013, **13**, 1764–1769; (*c*) A. Abrusci, S. D. Stranks, P. Docampo, H.-L. Yip, A. K. Y. Jen and H. J. Snaith, *Nano Lett.*, 2013, **3**, 3124–3128; (*d*) W. Zhang, B. Cai, Y. Xing, Z. Yang and J. Qiu, *Energy Environ. Sci.*, 2013, **6**, 1480–1485; (*e*) Y. S. Kwon, J. Lim, H.-J. Yun, Y.-H. Kim and T. Park, *Energy Environ. Sci.*, 2014, **7**, 1454–1460.

10 (*a*) D. Gendron and M. Leclerc, *Energy Environ. Sci.*, 2011, **4**, 1225–1237; (*b*) P. M. Beaujuge and J. M. J. Fréchet, *J. Am. Chem. Soc.*, 2011, **133**, 20009–20029.

11 (*a*) N. J. Jeon, J. Lee, J. H. Noh, M. K. Nazeeruddin, M. Grätzel and S. I. Seok, *J. Am. Chem. Soc.*, 2013, **135**, 19087–19090; (*b*) K. Thirumal, K. Fu, P. P. Boix, H. Li, T. M. Koh, W. Leong, S. Powar, A. C. Grimsdale, M. Gratzel, N. Mathews and S. G. Mhaisalkar, *J. Mater. Chem. A*, 2014, **2**, 6305–6309; (*c*) H. Li, K. Fu, A. Hagfeldt, M. Grätzel, S. G. Mhaisalkar and A. C. Grimsdale, *Angew. Chem., Int. Ed.*, 2014, **53**, 4085–4088.

12 C. Wetzel, A. Mishra, E. Mena-Osteritz, A. Liess, M. Stolte, F. Würthner and P. Bäuerle, *Org. Lett.*, 2014, **16**, 362–365.

13 K. Mitsudo, S. Shimohara, J. Mizoguchi, H. Mandai and S. Suga, *Org. Lett.*, 2012, **14**, 2702–2705.

14 A. Mishra, C. Uhrich, E. Reinold, M. Pfeiffer and P. Bäuerle, *Adv. Energy Mater.*, 2011, **1**, 265–273.

15 G. Rothenberger, D. Fitzmaurice and M. Grätzel, *J. Phys. Chem.*, 1992, **96**, 5983–5986.

16 J. H. Noh, N. J. Jeon, Y. C. Choi, M. K. Nazeeruddin, M. Grätzel and S. I. Seok, *J. Mater. Chem. A*, 2013, **1**, 11842–11847.